ISSN 1027-4510, Journal of Surface Investigation: X-ray, Synchrotron and Neutron Techniques, 2018, Vol. 12, No. 6, pp. 1077–1081. © Pleiades Publishing, Ltd., 2018.
Original Russian Text © S.M. Baraishuk, T.M. Tkachenko, A.V. Stanchik, V.F. Gremenok, S.A. Bashkirov, M. Wiertel, M. Budzynski, A.I. Turovets, Y.S. Yakovenko, 2018, published in Poverkhnost', 2018, No. 11, pp. 35–40.

Influence of the Substrate Type on the Surface Morphology of $Cu_2ZnSnSe_4$ Thin Films

S. M. Baraishuk[a], T. M. Tkachenko[a], A. V. Stanchik[b, *], V. F. Gremenok[b], S. A. Bashkirov[b], M. Wiertel[c], M. Budzynski[c], A. I. Turovets[d], and Y. S. Yakovenko[d]

[a] *Belarusian State Agrarian Technical University, Minsk, 220023 Belarus*
[b] *Scientific-Practical Center of Material Science, National Academy of Sciences of Belarus, Minsk, 220072 Belarus*
[c] *Maria Curie-Skłodowska University, 20-031 Lublin, Poland*
[d] *Tank Belarusian State Pedagogical University, Minsk, 220050 Belarus*
**e-mail: stanchik@physics.by*

Received February 10, 2018

Abstract—Investigations into the influence of the substrate type (a glass substrate with a molybdenum sublayer, tantalum and molybdenum foils) on the surface morphology of $Cu_2ZnSnSe_4$ thin films obtained by selenization of electrochemically deposited and preliminary annealed metallic precursors are presented. Metal foils are attractive for use as substrates of solar cells in both ground and space objects due to their light weight, flexibility, and the possibility of using the commercial roll-to-roll technology of film fabrication, leading to a reduction in the cost. At different stages of $Cu_2ZnSnSe_4$ film preparation, their surface morphology is studied by atomic-force microscopy and scanning electron microscopy in combination with energy-dispersive spectrometry. The metal substrate morphology is demonstrated to have an insignificant effect on the surface morphology of $Cu_2ZnSnSe_4$ films, indicating that flexible-foil substrates are promising for the production of thin-film solar cells.

Keywords: $Cu_2ZnSnSe_4$ thin films, precursors, flexible metal substrates, atomic-force microscopy, scanning electron microscopy

DOI: 10.1134/S1027451018050415

INTRODUCTION

Quaternary $Cu_2ZnSnSe_4$ (CZTSe) semiconductor compound is a promising material for thin-film solar cells due to the corresponding band-gap (1.0 eV), a high radiation absorption coefficient in the visible range (more than 10^4 cm^{-1}), and *p*–type conductivity [1, 2]. In contrast to $CuIn_{1-x}Ga_xSe_2$ and CdTe materials, which are applied at present, CZTSe contains earth-abundant, low-cost and nontoxic components [2–4]. The maximum attainable photoelectric-conversion efficiency of CZTSe solar cells is ~30% [5].

The electrochemical deposition technique has several advantages over other methods enabling the preparation of CZTSe thin films: the thickness and morphology of the films can be controlled by adjusting the electrochemical parameters, and film production is economically profitable because there is no need for high vacuum, powerful supply sources, and high reaction temperatures [6]. CZTSe-based thin film solar cells obtained by electrochemical deposition have 7% power conversion efficiency [7]. This indicates that the given fabrication method is competitive from viewpoints of both cost and efficiency.

The advantages of solar panels on flexible metal substrates are obvious, namely, light weight, flexibility, and strength, especially in the fields of their application, such as outer space, aviation, electric cars, textile goods, portable electronics, and so forth [8]. Foil substrates make it possible to employ roll-to-roll technologies of film production ensuring a continuous process of their deposition at high rates and exclude the necessity of depositing a conducting back layer, thereby substantially decreasing the cost of solar panel fabrication.

However, in contrast to glass substrates, metal foils have rougher surfaces, which strongly affect crystal growth and its orientation and, consequently, the solar cell power conversion efficiency [9]. The purpose of this work is to reveal the regularities underlying the influence of the substrate type (glass substrate with a molybdenum sublayer (or Mo/glass substrate) and Mo and Ta foils) on the surface morphology of CZTSe thin films.

EXPERIMENTAL

CZTSe thin films were prepared by the selenization of preliminarily annealed Cu–Zn–Sn (CZT) precur-

Table 1. Arithmetical mean (R_a) and root-mean-square (R_q) roughnesses of the substrate, precursor, and film surfaces

Substrate type	Mo/glass		Mo foil		Ta foil	
parameters	R_a, nm	R_q, nm	R_a, nm	R_q, nm	R_a, nm	R_q, nm
Substrate	8.15	9.95	144.21	178.36	68.66	88.48
Deposited CZT precursor	80.80	109.60	273.00	335.20	225.48	282.81
Preliminarily annealed CZT precursor	162.06	208.52	44.89	58.49	31.60	40.50
CZTSe film	209.48	262.38	204.50	268.10	187.03	244.43

sors, which were electrochemically deposited onto a Mo/glass substrate and Mo and Ta foils. Before CZT precursor deposition, the Mo and Ta substrates were mechanically treated. Afterward, the metal substrates, as well as the Mo/glass one, were washed in alcohol and distilled water with subsequent drying in hot air. CZT precursors were deposited layer-by-layer, and the layered sequence was Cu/Sn/Cu/Zn. The anodes were wafers of commercial anodic copper, high-purity (99.999%) tin, and zinc. Electrolyte solutions were prepared using sulfate solutions of the corresponding metals. The obtained CZT precursors on metal Mo and Ta foils were polished by an industrial Ultracut (Poland) K2 polishing paste to remove the hydroxide layer from the surface and washed with acetone and distilled water.

Preliminary annealing of the deposited CZT precursors was carried out in a 95% Ar + 5% H_2 atmosphere at a temperature of 350°C for 30 min. The annealed CZT precursors were selenized in a quartz container (its volume was 5 cm^3) with 13 mg of powder-like Se at an Ar pressure of 1 bar and a temperature of 580°C for 30 min.

CZT precursor and CZTSe film surfaces were investigated using a Microtestmachines NT 206 atomic-force microscope operating in the contact mode. To estimate the surface, no less than five scanning areas with sizes of 10 × 10 μm were chosen in different surface regions, enabling averaging of the relief parameters. The chemical composition of the CZTSe films was determined by energy-dispersive X-ray spectrometry using an Oxford Instruments Aztec Energy-Advanced EDX electron-probe microscope equipped with an X-act silicon-drift detector (the active crystal area is 10 mm^2) and operating at room temperature. The primary ion-beam energy was 20 keV. The surface morphology of CZT precursors and CZTSe films were investigated by scanning electron microscopy (SEM) using a TESCAN Vega 3LMU electron microscope with an Everhart-Thornley secondary-electron detector (yttrium–aluminum garnet crystal).

RESULTS AND DISCUSSION

Atomic-force microscopy (AFM) studies demonstrated that CZT precursor surfaces (Figs. 1b, 1c) deposited onto Mo and Ta foils substrates have similar microreliefs and differ from that observed on the Mo/glass substrate (Fig. 1a) [10, 11].

The surface of the CZT precursor on the Mo/glass substrate (Fig. 1a) is characterized by a local granular structure. In this case, the sizes and height of large agglomerates are 2 × 4 μm and 150–200 nm, respectively, and small grains are rounded and have sizes of about 300 × 300 nm at a height of 15–20 nm. SEM confirms that the CZT precursor surface contains microscale agglomerates (Fig. 2a). The SEM image shows a region of the initial surface of the Mo/glass substrate (the lower right corner) and the structure formed on the substrate surface due to CZT precursor electrodeposition.

The surface of CZT precursors deposited onto metal substrates is defined by a complex granular structure (Figs. 1b, 1c). When the CZT precursor is situated on a molybdenum foil, its surface incorporates nanoscale rounded and prolate agglomerates with sizes of (50–100) × (200–400) nm, which are oriented along a single direction. In the case of the CZT precursor located on the tantalum foil, the size of the observed rounded grains varies from 250 to 1000 nm in the transverse section. The grains are also combined into larger structures on the CZT precursor surface observed on the tantalum foil. In this case, the generated cavities are larger than those corresponding to the precursor on Mo foil, increasing the roughness up to 200 nm and higher (Table 1). In accordance with the SEM data, the cavities observed on the CZT precursor surface can be attributed to cracks (Fig. 2b) formed during hydroxide-layer removal from the surface.

It is seen from the data of Table 1 that molybdenum and tantalum substrates have a higher roughness than that of the Mo/glass substrate because of mechanical treatment. The surface roughness of CZT precursors on the Mo/glass substrate increased by a factor of 8–10 as compared to the substrate. This can be explained by the influence of large surface clusters of the deposited CZT precursor (Fig. 1a). At the same time, CZT precursors on Mo and Ta foil substrates are characterized by the fact that the roughness increases by a factor of 2–3 as compared to the substrate one. However, the roughness of the CZT precursors on metal substrates exceeds the values inherent to the Mo/glass substrate. This evidences the fact that the

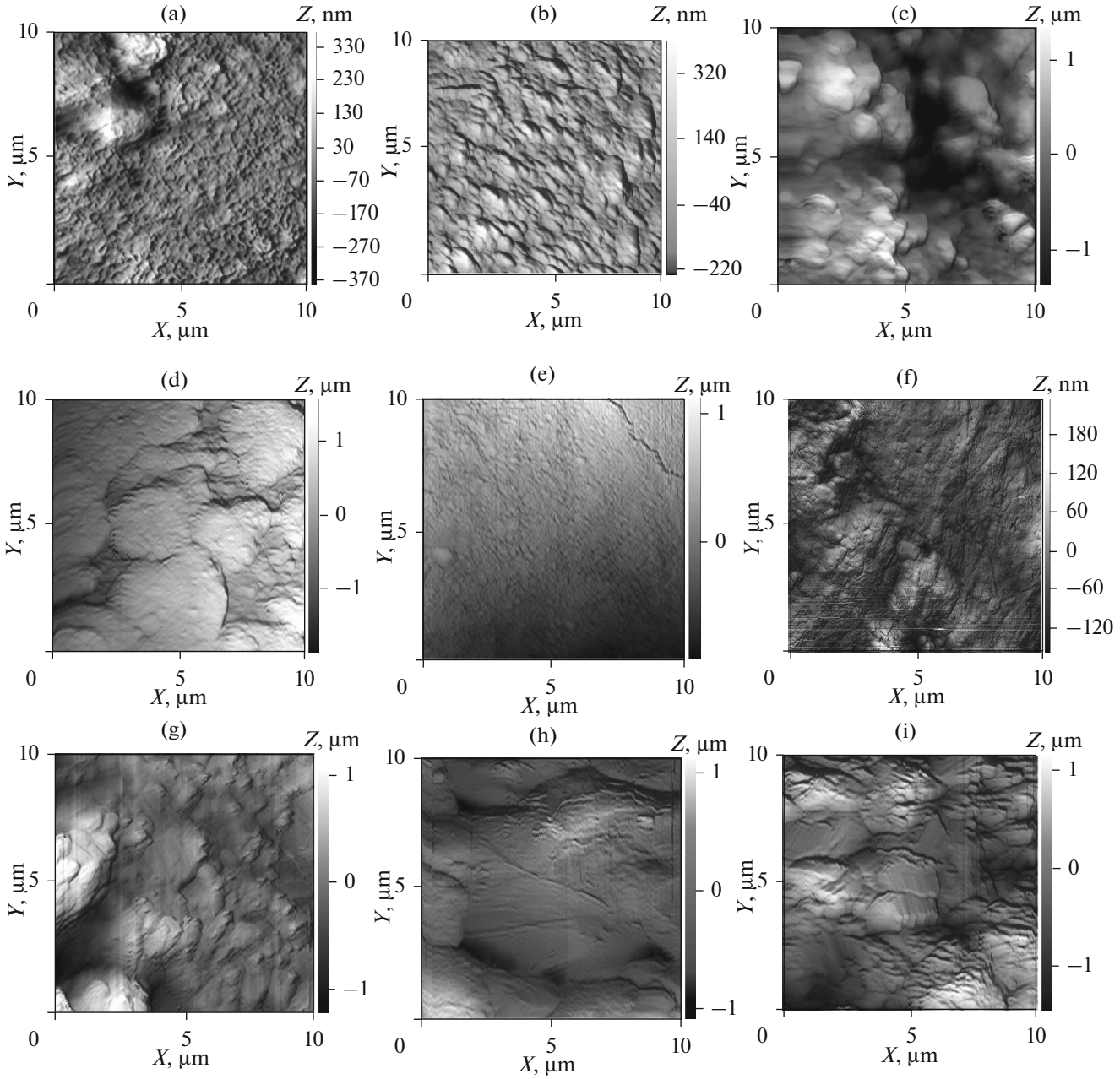

Fig. 1. Typical AFM surface images of (a–c) electrically deposited and (d–f) preliminarily annealed CZT precursors and (g–i) CZTSe films on (a, d, g) Mo/glass substrates and (b, e, h) Mo and (c, f, i) Ta foils.

metal-substrate surface affects the formation of the surface morphology of precursors.

After preliminary annealing in an argon atmosphere, the surface morphology of CZT precursors considerably changed for all substrates (Figs. 1d–1f). In the case of the CZT precursor on a Mo/glass substrate, the grain size increased to 0.28–4 μm, and, simultaneously, the height gradient grew, increasing the precursor surface roughness. On the contrary, the CZT precursor surface on metal substrates became more homogeneous, and the roughnesses decreased appreciably as compared to the deposited CZT precursors. A set of small-grained aggregates is observed on the surface of the CZT precursor on the tantalum foil. Undoubtedly, this corresponds to growing grains emerging from the CZT precursor surface. All these results unambiguously indicate that, after preliminary annealing, changes in the surface morphology of CZT precursors are caused by both grain growth and material agglomeration.

AFM studies demonstrated that a granular structure was formed on the surface of CZTSe films on all

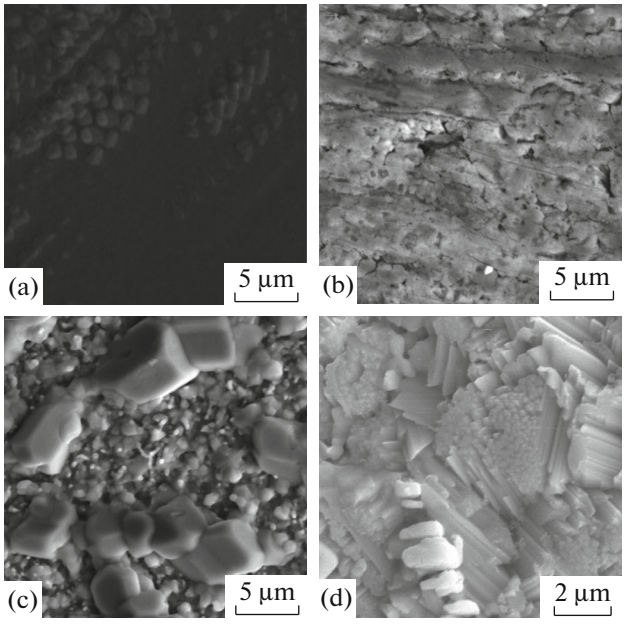

Fig. 2. Typical SEM surface images of CZT precursors electrically deposited onto (a) Mo/glass and (b) Mo foil substrates and CZTSe films deposited onto (c) Mo and (d) Ta foils.

types of substrates, namely, Mo/glass substrates and Mo and Ta foils (Figs. 1g–1i). It is possible to distinguish two types (large and small) of grains on the CZT precursor surfaces located on Mo/glass and Mo foil substrates. The grain sizes typical of CZTSe films on the Mo/glass substrate are 400 × 200 and 270 × 130 nm at heights of 160–194 nm. In the case of the film on the Mo foil, the grain sizes are 6 × 7.2 and 1 × 1.1 μm, respectively, and their heights are approximately identical: ~280 nm. This agrees well with the parameters calculated according to SEM images (Fig. 2c). When the CZTSe film is deposited onto the Ta foil, a layered structure composed of 2–3-μm-long agglomerates with a cross section of 200 × 250 nm is generated. They are packed in the form of "blocks" and located arbitrarily with respect to each other. Such a structure of the CZTSe film surface was determined by combining the scanning probe and electron microscopy techniques. This made it possible to estimate its parameters and perform surface visualization (Fig. 2d). In accordance with [12], when the film selenization pressure is high, the layer thickness increases, the grain morphology becomes more pronounced, and angular boundaries between grains are formed. This agrees with the aforementioned results.

It is apparent from Figs. 1g–1i that cracks and micropores are lacking on the CZTSe film surface on all types of substrates. This indicates the high compactness and homogeneity of the CZTSe layer, which arise from further grain growth and material agglomeration. In all cases, the average size of CZTSe film grains tends to increase, thereby increasing the surface roughness of films as compared to the CZT precursors (Table 1).

The roughness parameters of the CZTSe films deposited on the Mo/glass and metal substrates unexpectedly differ little although foil substrates were primarily characterized by higher roughnesses, defects in the form of scratches, and the different surface morphologies of the precursors after preliminarily annealing. Hence, the surface morphology of the metal substrates insignificantly affects the micro- and nanoreliefs of the thin films. This agrees well with the data from [13, 14].

The chemical composition of the CZTSe films on a Mo/glass, Mo and Ta foil substrates (Table 2) indicates enrichment with zinc, corresponding to the criterion of highly effective thin-film solar cells based on CZTSe films [1]. In accordance with [15, 16], the CZTSe films enriched with zinc are characterized by the fact that large $Cu_2ZnSnSe_4$ crystals begin to grow, a compact layer is formed, and excessive zinc remains on the surface. As a consequence, small crystallites of zinc selenide are generated. This agrees well with AFM data for CZTSe films (Figs. 1g–1i). It is likely that when CZTSe films on Mo/glass and Mo foil substrates are enriched with copper, the copper selenide phase is created. For example, large crystals whose shape is typical of copper selenide are observed on the SEM surface image of the CZTSe film on the molybdenum foil (Fig. 2c) [17, 18]. The X-ray spectrum of the CZTSe film on the Mo foil (Fig. 3) includes peaks corresponding to copper, zinc, tin, and selenium, and less intense peaks that can be attributed to the substrate. On average, the CZTSe film composition is homogeneous over the entire surface. Selenium is predominant in the obtained X-ray spectrum of the CZTSe film. Moreover, the mass dominance of zinc over tin is observed. Therefore, calculations of the

Table 2. Chemical composition of the CZTSe films on different substrates

Substrate type	Cu		Zn		Sn		Se	
	wt %	at %	wt %	at %	wt %	at %	wt %	at %
Mo/glass	27.96	32.77	12.25	13.95	9.84	6.17	49.95	47.11
Mo foil	26.50	31.15	13.07	14.93	10.29	6.48	50.14	47.44
Ta foil	20.86	25.61	10.80	12.88	18.15	11.93	50.19	49.58

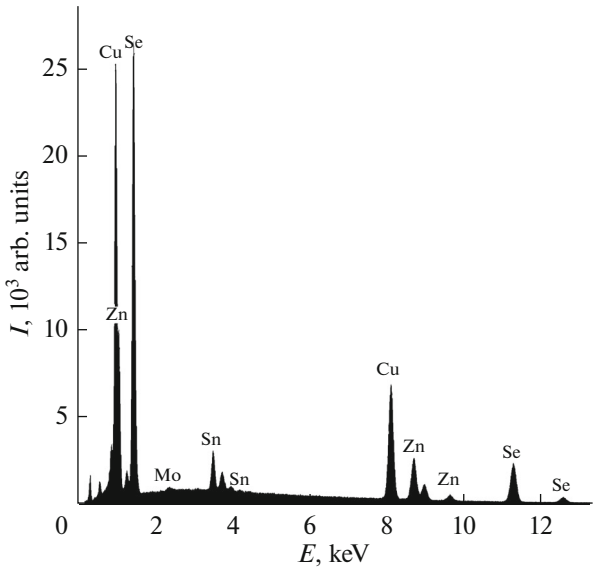

Fig. 3. Typical X-ray spectrum of the CZTSe film onto Mo foil substrates.

chemical composition of the films are confirmed (Table 2). Analogous spectra were constructed for CZTSe films on Mo/glass and Ta foil substrates.

CONCLUSIONS

The $Cu_2ZnSnSe_4$ thin films are prepared by selenizing layerwise electrochemically deposited and preliminarily annealed Cu–Zn–Sn precursors on the Mo/glass substrate and flexible metal Mo and Ta foil substrates. It is demonstrated that the substrate type affects the surface morphology of CZT precursors. Preliminary annealing of the deposited CZT precursors substantially changes the surface morphology. After preliminary annealing, the surface roughness of the CZT precursor on the Mo/glass and metal substrates increases and decreases, respectively. In all cases, a granular structure is formed on the CZTSe film surfaces. An increase in the CZTSe film roughness is caused by grain growth during selenization. The CZTSe films on a glass substrate with a molybdenum sublayer and on metal foils have close roughnesses. This indicates that flexible metal foils can be employed as substrates for thin-film solar cells. The chemical composition of the CZTSe films determined by energy-dispersive spectroscopy has no unwanted components within the limits of method sensitivity.

In the near future, the obtained data will be used to develop technology for preparing CZTSe thin films on flexible metal substrates and create solar cells on their basis.

ACKNOWLEDGMENTS

This work was performed in the context of scientific research according to the grant of the National Academy of Sciences of Belarus, by the State program of scientific studies “Physical Material Science, New Materials and Technologies” (MATTEX 1.0.6), and was supported by the Belarusian Republican Foundation for Fundamental Research (project no. F17PM-089).

REFERENCES

1. *Semiconductor Materials for Solar Photovoltaic Cells* Ed. by M. P. Paranthaman, W. Wong-Ng, and R. N. Bhattacharya, Vol. 218 of *Springer Series in Material Science* (Springer, 2016).
2. M. A. Green, K. Emery, Y. Hishikawa, et al., Prog. Photovoltaics. **24**, 905 (2016). doi 10.1002/pip.2788
3. M. A. Green, Prog. Photovoltaics. **17**, 347 (2009). doi 10.1002/pip.899
4. P. D. Moskowitz and V. M. Fthenakis, Sol. Cells **29**, 63 (1990).
5. W. Shockley and H. J. Queisser, J. Appl. Phys. **32**, 510 (1961). doi 10.1063/1.1736034
6. J. Lee, S. C. Nam, and Y. Tak, Korean J. Chem. Eng. **22**, 161 (2005). doi 10.1007/BF02701479
7. L. Guo, Y. Zhu, O. Gunawan, et al., Prog. Photovoltaics. **22**, 58 (2012). doi 10.1002/pip.2332
8. M. Pagliaro, G. Palmisano, and R. Ciriminna, *Flexible Solar Cells* (Wiley, Weinheim, 2008).
9. F. Kessler and D. Rudmann, Sol. Energy **77**, 685 (2004). doi 10.1016/j.solener.2004.04.010
10. A. V. Stanchik, S. A. Bashkirov, Y. S. Yakovenko, et al., Fiz. Obraz. VUZakh **22** (1), 106C (2016).
11. A. V. Stanchik, S. M. Barajshuk, S. A. Bashkirov, et al., Vestsi Nats. Akad. Nauk Belarusi., Ser. Fiz.-Mat. Nauk, No. 4, 67 (2016).
12. H. Chia-Ho and W. Dong-Cherng, Int. J. Photoenergy **2014**, 568648 (2014). doi 10.1155/2014/568648
13. I. S. Tashlykov and S. M. Baraishuk, Russ. J. Non-Ferrous Met. **49**, 303 (2008). doi 10.3103/S1067821208040172
14. I. Tashlykov, S. Baraishuk, O. Mikkalkovich, and I. Antonovich, Przegl. Elektrotech. **84** (3), 111 (2008).
15. R. Kondrotas, A. Juskenas, A. Naujokaitis, et al., Sol. Energy Mater. Sol. Cells **132**, 21 (2015). doi 10.1016/j.solmat.2014.08.010
16. A. Redinger, K. Hönes, X. Fontané, et al., Appl. Phys. Lett. **98**, 101907 (2011). doi 10.1063/1.3558706
17. A. H. Pinto, S. W. Shin, E. S. Aydil, and R. L. Penn, Green Chem. **18**, 5814 (2016). doi 10.1039/c6gc01287f
18. C. Xue, D. Papadimitriou, Y. S. Raptis, et al., J. Appl. Phys. **96**, 1963 (2004). doi 10.1063/1.1772885

Translated by S. Rodikov